

PROKR2 missense mutations associated with Kallmann syndrome impair receptor signalling activity

Carine Monnier^{1,†}, Catherine Dodé^{2,†}, Ludovic Fabre¹, Luis Teixeira², Gilles Labesse⁴, Jean-Philippe Pin¹, Jean-Pierre Hardelin^{3,*} and Philippe Rondard¹

¹CNRS UMR5203, Institut de Génomique Fonctionnelle, INSERM U661, Université Montpellier 1,2, Montpellier, France, ²INSERM U567, Département de Génétique et Développement, Institut Cochin, Université Paris-Descartes, Paris, France, ³INSERM UMRS587, Département de Neurosciences, Institut Pasteur, UPMC Paris 06, Paris, France and ⁴Atelier de Bio- et Chimie-Informatique Structurale, Centre de Biochimie Structurale CNRS UMR5048, INSERM U554, Université Montpellier 1,2, Montpellier, France

Received June 6, 2008; Revised and Accepted September 26, 2008

Kallmann syndrome (KS) combines hypogonadism due to gonadotropin-releasing hormone deficiency, and anosmia or hyposmia, related to defective olfactory bulb morphogenesis. In a large series of KS patients, ten different missense mutations (p.R85C, p.R85H, p.R164Q, p.L173R, p.W178S, p.Q210R, p.R268C, p.P290S, p.M323I, p.V331M) have been identified in the gene encoding the G protein-coupled receptor prokineticin receptor-2 (PROKR2), most often in the heterozygous state. Many of these mutations were, however, also found in clinically unaffected individuals, thus raising the question of their actual implication in the KS phenotype. We reproduced each of the ten mutations in a recombinant murine Prokr2, and tested their effects on the signalling activity in transfected HEK-293 cells, by measuring intracellular calcium release upon ligand-activation of the receptor. We found that all mutated receptors except one (M323I) had decreased signalling activities. These could be explained by different defective mechanisms. Three mutations (L173R, W178S, P290S) impaired cell surface-targeting of the receptor. One mutation (Q210R) abolished ligand-binding. Finally, five mutations (R85C, R85H, R164Q, R268C, V331M) presumably impaired G protein-coupling of the receptor. In addition, when wild-type and mutant receptors were coexpressed in HEK-293 cells, none of the mutant receptors that were retained within the cells did affect cell surface-targeting of the wild-type receptor, and none of the mutant receptors properly addressed at the plasma membrane did affect wild-type receptor signalling activity. This argues against a dominant negative effect of the mutations *in vivo*.

INTRODUCTION

Kallmann syndrome (KS) is a developmental disease that combines hypogonadotropic hypogonadism, due to gonadotropin-releasing hormone (GnRH) deficiency, and anosmia or hyposmia, related to the absence or hypoplasia of the olfactory bulbs and tracts. KS is genetically heterogeneous. Five causal genes have been identified so far, namely *KALI*, *FGFR1*, *FGF8*, *PROKR2* and *PROK2*, encoding the extracellular glycoprotein anosmin-1, fibroblast growth factor receptor-1, fibroblast growth factor-8, prokineticin

receptor-2 (a G protein-coupled receptor of class A, 1) and prokineticin-2, respectively (see 2 for review). Loss-of-function mutations in *KALI* and in *FGFR1* or *FGF8* underlie the X-linked recessive form of the disease and an autosomal dominant form with incomplete penetrance, respectively (3–6). *PROKR2* and *PROK2* have been identified by a candidate gene approach based on the phenotypes of the corresponding knock-out mice (7). Indeed, prokineticin receptor-2 null and prokineticin-2 null mice both display KS-like features, namely olfactory bulb morphogenetic defects and a severe atrophy of the reproductive system

*To whom correspondence should be addressed. Email: jean-pierre.hardelin@pasteur.fr

†These authors contributed equally to this work.

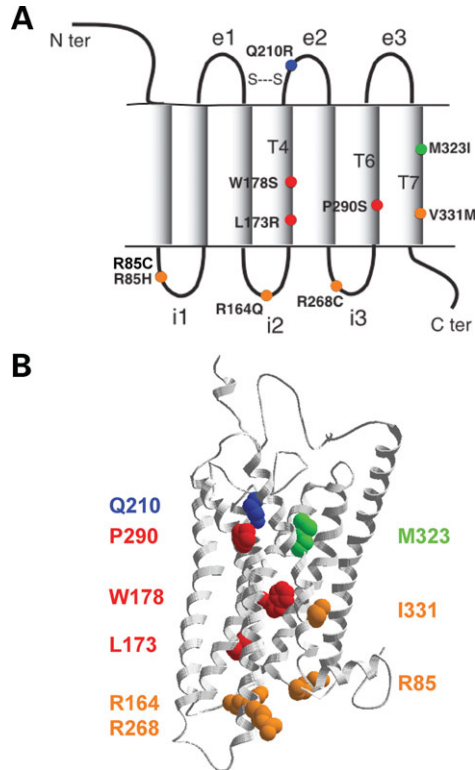


Figure 1. (A) Schematic representation of the human PROKR2. Missense mutations that impaired cell surface expression (red), ligand binding (blue), or G-protein coupling (orange), and the mutation that did not affect receptor signalling activity (green) are indicated. T1–T7, i1–i3 and e1–e3 denote the seven transmembrane domains, three intracellular loops and three extracellular loops of the receptor, respectively. (B) Structural model of the murine Prokr2. Ribbon views of the receptor with the residues mutated in KS patients indicated in Corey–Pauling–Koltun representation, according to the colours in (A). All the amino acid residues affected by the human mutations are identical in the mouse protein, except at position 331 where the human valine residue is replaced by isoleucine in the mouse.

related to markedly reduced numbers of GnRH-synthesizing cells in the hypothalamus (8–10).

The first mutations in *PROKR2* were found in 14 out of 192 independent KS patients, either in heterozygous state (10 patients) or in homozygous (or compound heterozygous) state (4 patients). Notably, of the ten different mutations identified, only one was a frame-shifting mutation (p.20fsX43), while nine were missense mutations (p.R85H, p.R164Q, p.L173R, p.W178S, p.Q210R, p.R268C, p.P290S, p.M323I, p.V331M; see Fig. 1A). Moreover, three missense mutations present in heterozygous state in KS patients (R268C, P290S, V331M) and two additional missense mutations not found in the initial cohort of KS patients were detected in control individuals from the general population (7). Since then, one of the latter mutations (p.R85C) has also been found in individuals affected by KS or isolated hypogonadotropic hypogonadism (C.D., unpublished data and 11). This raises the question of the pathogenic role of the various *PROKR2* missense mutations in KS. Here, we address this issue by means of two complementary approaches. Firstly, we took advantage of the crystal structures of rhodopsin and the β 2-adrenergic receptor, two G protein-coupled receptors (GPCRs) belonging

to the same subfamily as PROKR2 (1), to build a three-dimensional model of PROKR2 and predict how each of the ten missense mutations identified in KS patients could affect the structure and functioning of the receptor. Secondly, we tested the functional effect of each of these mutations reproduced by site-directed mutagenesis, on PROKR2 signalling in transfected HEK-293 cells.

RESULTS AND DISCUSSION

Bioinformatic prediction of the functional consequences of the mutations

We used the three-dimensional structures of the bovine rhodopsin (12,13) and human β 2 adrenergic receptor (14,15) to build a homology model of the murine Prokr2 (Fig. 1B). Based on this model, the non-conservative W178S, L173R and P290S mutations that affect residues within PROKR2 transmembrane domains are predicted to impair stability or correct folding of the receptor, and consequently its cell surface-targeting. Indeed, Trp178 and Pro290 are the most conserved residues of transmembrane domains 4 and 6, respectively (positions 4.50 and 6.50, according to the Ballessteros and Weinstein nomenclature, 16), and Leu173 is in a hydrophobic environment that would not easily put up with a positively charged arginine residue. The Q210R mutation, affecting a residue located in extracellular loop 2, may impair ligand-binding of the receptor. The four mutations affecting arginine residues in the intracellular loops (R85C, R85H, R164Q and R268C) could influence G protein activation. Finally, the M323I and V331M conservative mutations located in transmembrane domain 7 are predicted to have limited impact on the receptor properties. To test these predictions, we reproduced each mutation in a recombinant haemagglutinin (HA)-tagged mouse Prokr2 by site-directed mutagenesis, and measured the PROKR2-evoked signalling activity, cell surface amount and agonist-binding of the mutant receptors.

All *PROKR2* missense mutations except one impair intracellular Ca^{2+} increase evoked by PROKR2

PROKR2 is a Gq-coupled receptor that promotes inositol-phosphate production, and intracellular Ca^{2+} mobilization (17–19). We analyzed the signalling activity of the HA-tagged Prokr2 mutants by measuring the intracellular release of Ca^{2+} induced by the ligand PROKR2. We found that the signalling activity of all mutants except one (M323I) was impaired, as indicated by the right shift of the agonist dose–response curves, and the decreased maximal responses (Fig. 2A and Table 1). Mutations P290S, W178S, Q210R and R164Q had the most deleterious effects on Ca^{2+} release. Our results are consistent with those recently obtained by Cole *et al.* (11), who also studied the deleterious effect of ten *PROKR2* missense mutations on intracellular Ca^{2+} mobilization, including the R85C, R164Q, L173R, W178S and V331M mutations analyzed here. Western blot analysis of the transfected HEK-293 cells showed that all mutant receptors were produced in similar amounts, and with the expected molecular weight for a SDS-resistant dimeric form (~ 80 kDa) (Fig. 2B).

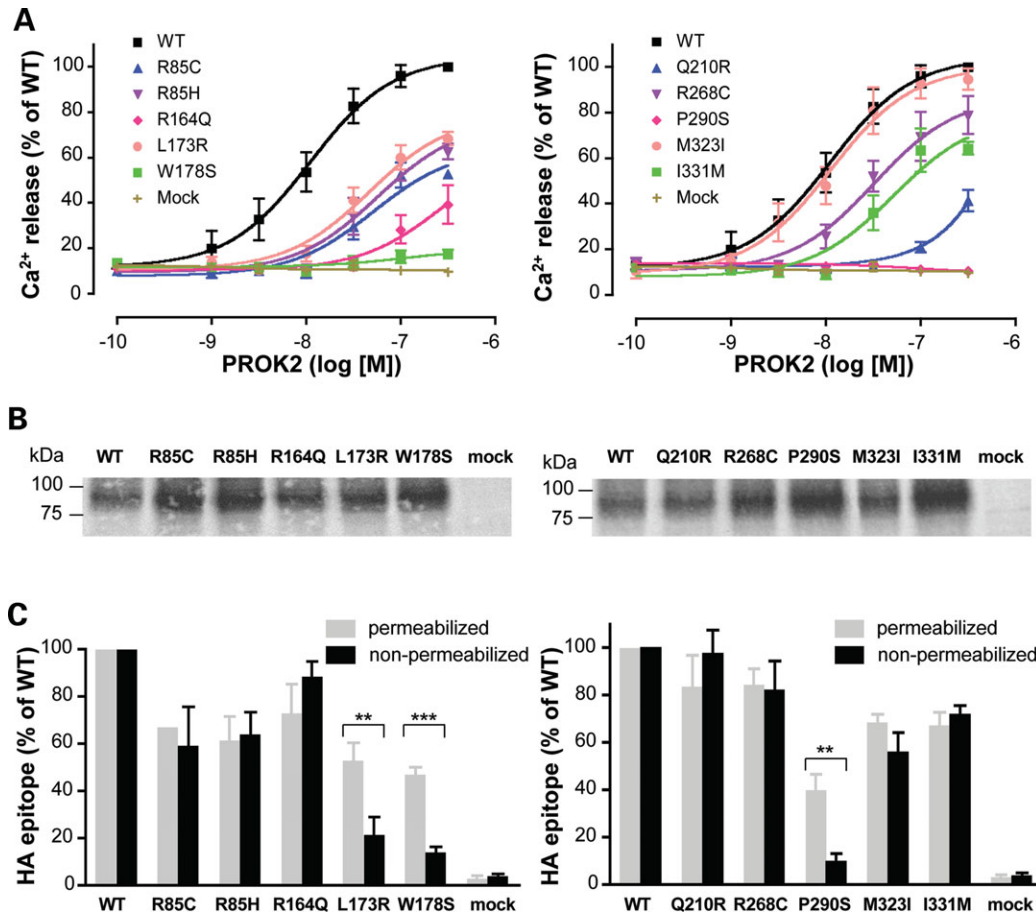


Figure 2. Functional analysis of the HA-tagged Prokr2 mutants. (A) Intracellular Ca²⁺ response mediated by the wild-type and mutant HA-tagged Prokr2. Data are means \pm SEM of at least three independent experiments. Differences between the wild-type and mutant receptors are all statistically significant (Student's *t*-test, $P < 0.001$), except for the M323I mutant ($P > 0.05$). (B) Western blot analysis of the wild-type and mutant HA-Prokr2 in membrane fractions of cells. (C) Surface and total cell levels of the Prokr2 mutants at the cell surface (non-permeabilized cells, black histograms) and in permeabilized cells (grey histograms) were quantified by ELISA. Data are means \pm SEM of at least three independent experiments. * $P < 0.05$, ** $P < 0.01$ and *** $P < 0.001$ (Student's *t*-test).

Table 1. Functional characterization of Prokr2 mutants in transfected HEK-293 cells

Prokr2	Cell surface amount ^a (% of WT)	Ligand binding ^b IC ₅₀ \pm SEM (nM)	Signalling activity ^c EC ₅₀ \pm SEM (nM)
Wild-type	100	17.7 \pm 3.6	15.9 \pm 3.9
R85C	59.3 \pm 16.4	13.0 \pm 2.3	81.8 \pm 22.7
R85H	64.0 \pm 9.5	18.9 \pm 8.0	95.1 \pm 34.9
R164Q	88.5 \pm 6.5	13.4 \pm 2.2	ND
L173R	21.6 \pm 7.5	ND	63.5 \pm 20.7
W178S	14.2 \pm 2.1	ND	ND
Q210R	97.6 \pm 9.8	ND	ND
R268C	82.2 \pm 12.0	12.5 \pm 2.3	40.9 \pm 11.1
P290S	9.9 \pm 3.3	ND	ND
M323I	56.1 \pm 8.1	22.3 \pm 4.1	10.1 \pm 4.9
I331M	71.9 \pm 3.8	13.1 \pm 4.0	60.2 \pm 20.7

ND, not determined.

^aELISA.

^bDisplacement of ¹²⁵I-MIT-1 by PROK2.

^cIntracellular calcium release upon stimulation by PROK2.

The M323I mutation has so far been found only in compound heterozygous KS patients, together with a deleterious frame-shifting mutation (7). Based on the present results, this conservative missense mutation may not be considered pathogenic, although the possibility that it affects a Ca²⁺-independent PROKR2 signalling pathway, not explored in this study, should not be excluded (11).

Transmembrane domain mutations L173R, W178S and P290S impair cell surface-targeting of the receptor

The amount of receptor present in the plasma membrane was estimated for each mutated Prokr2 by means of ELISA quantification in intact (i.e. non-permeabilized) cells, using the HA epitope at the extracellular N-terminal end of the receptor (see Materials and Methods). Seven out of ten mutant receptors were found in substantial amounts (>50% of the wild-type receptor amount) at the cell surface. In contrast, the L173R, W178S and P290S receptors had low cell

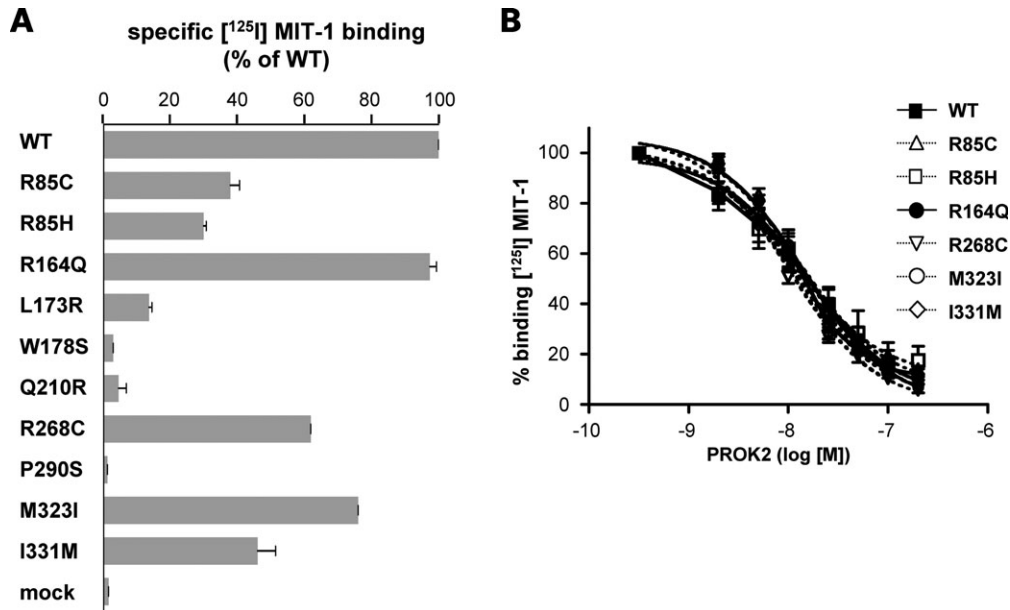


Figure 3. Ligand-binding properties of Prokr2 mutants. (A) Specific binding of ^{125}I -MIT-1 to wild-type and mutant Prokr2. Bound radioligand was displaced in the presence of 200 nM PROK2. Data are means \pm SEM of at least three independent measurements. (B) Displacement of non-permeant agonist ^{125}I -MIT-1 by PROK2 on HA-tagged wild-type and six mutant Prokr2. Data are means \pm SEM of at least three independent experiments.

surface levels (Fig. 2C and Table 1) despite quite large total cell amounts (see Fig. 2B), thus suggesting that these mutants had difficulties passing the quality control system. This was confirmed by the quantification of total protein levels by ELISA in permeabilized cells. Concomitant ELISA quantifications in permeabilized and non-permeabilized cells also showed that the other mutant receptors were correctly addressed to the cell surface (Fig. 2C). Notably, although similar low levels of the L173R, W178S and P290S receptors were detected at the cell surface, the L173R receptor was still able to evoke intracellular Ca^{2+} release upon ligand-activation, whereas the W178S and P290S receptors were not (see Fig. 2A and C). This indicates that the W178S and P290S mutations not only impair cell surface-targeting of the receptor, but also its ability to activate the Gq protein.

Extracellular loop mutation Q210R abolishes ligand-binding

Because the impaired signalling activity of some mutated receptors could be due to a decreased affinity for the ligand PROK2, we carried out binding experiments with the mutant receptors to measure agonist affinity. In these experiments, we used the high affinity and non-permeant agonist ^{125}I -mamba intestinal toxin-1 (MIT-1), which shows 60% of sequence identity with PROK2, and contains the functionally essential N-terminal motif AVITGA (20). As expected, ^{125}I -MIT-1 binding could not be detected with cells producing the W178S and P290S receptors that are not properly targeted to the plasma membrane (Fig. 3A). Notably, ^{125}I -MIT-1 did not bind to the Q210R receptor either, despite its normal expression at the cell surface (see Figs 2C and 3A). The other mutants displayed normal affinities for PROK2 as indicated by a competition experiment (Fig. 3B and Table 1).

Intracellular loop mutations R85C, R85H, R164Q, R268C and transmembrane domain mutation V331M presumably impair G protein-coupling

The four mutations located in PROKR2 intracellular loops (R85C, R85H, R164Q and R268C) and the murine I331M mutation (standing in for the V331M human mutation) located in the seventh transmembrane domain impaired receptor signalling upon agonist-stimulation, with R164Q (second intracellular loop) having the most severe effect (see Fig. 2A). The deleterious effect of these mutations could not be explained by impaired cell surface-targeting of the mutant receptors (see Fig. 2C) or impaired agonist affinity (see Fig. 3B). These mutations are thus likely to impair G protein-coupling of the receptor.

Mutant receptors do not exert a dominant negative effect on the wild-type receptor in co-transfected HEK-293 cells

Prokr2 knock-out mice display an abnormal, KS-like phenotype only in the homozygous state (9). Most KS patients carrying mutations in *PROKR2* are, however, heterozygous. We reasoned that the pathogenic effect of some of the *PROKR2* missense mutations found in heterozygous state could result from intracellular retention of the wild-type receptor by the mutant one, that is a dominant negative effect similar to that reported for other GPCRs (21–23). To determine if the L173R, W178S and P290S receptors that failed to reach the plasma membrane could exert such a dominant negative effect, we measured the amounts of wild-type receptor at the cell surface and in the whole cell, by means of ELISA without and with cell permeabilization, respectively, in co-transfected HEK-293 cells producing both Flag-tagged wild-type and HA-tagged mutant receptors. We found that cell surface-targeting of the wild-type receptor was not affected by any of these three mutants (Fig. 4A).

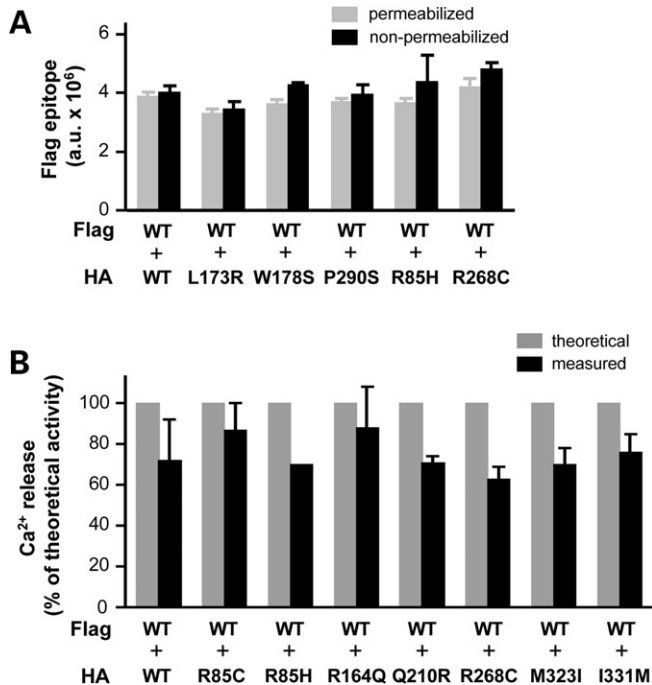


Figure 4. (A) Cell surface-targeting of wild-type receptors in the presence of mutant receptors. Total (grey histograms) and cell surface (black histograms) amounts of the Flag-tagged wild-type Prokr2 are determined by means of ELISA (arbitrary units, a.u.) with (permeabilized) and without (non-permeabilized) cell permeabilization, respectively, in the presence of HA-tagged wild-type or mutant Prokr2 (co-transfected HEK-293 cells). Data are means \pm SEM of triplicate determinations from a typical experiment repeated five times. A significant difference is not detected for any of the mutants studied, i.e. those that are properly addressed to the cell surface (R85H, R268C) and those that are not (L173R, W178S, P290S) (Student's *t*-test, $P > 0.05$). (B) Functional analysis of Prokr2 signalling activity when wild-type and mutant receptors are coexpressed. The intracellular Ca^{2+} responses mediated by the coexpressed Flag-tagged wild-type Prokr2 and HA-tagged wild-type or mutant Prokr2, upon 300 nM PROK2 stimulation, are shown for each of the seven mutant receptors that are properly targeted to the plasma membrane and for the wild-type receptor. For each pair of coexpressed receptors, the measured intracellular Ca^{2+} response (black histograms) is represented as the proportion of the expected calcium response if the two coexpressed receptors do not affect the signalling activity of each other (grey histograms). This theoretical value was calculated for every pair of coexpressed receptors, by adding the expected contributions of each receptor to the overall signalling activity according to its amount at the cell surface (see Materials and methods). Data are means \pm SEM of four independent experiments. A significant difference is not detected between the HA-tagged wild-type and any of the mutant receptors (Student's *t*-test, $P > 0.05$).

We then endeavoured to determine if some of the mutant receptors that are properly targeted to the plasma membrane could have a dominant negative effect on the receptor signalling activity. The calcium response to 300 nM PROK2 was measured upon coexpression of Flag-tagged wild-type Prokr2 and HA-tagged mutant Prokr2 in HEK-293 cells, and compared with the value that would be expected if the two coexpressed receptors do not affect the signalling activity of each other. Even though measured calcium responses were usually lower than the theoretical values, presumably due to saturation of the calcium signal (see Supplementary Material, Fig. S1), a significant difference in the response could not be detected between the HA-tagged wild-type and any of the mutant receptors upon coexpression with the Flag-tagged wild-type receptor (Fig. 4B).

Taken together, our results argue against a dominant negative effect of these mutations *in vivo*, and therefore support the current hypothesis of a digenic or oligogenic inheritance of KS in patients heterozygous for *PROKR2* mutations (24). Indeed, many of the mutations have also been found in clinically unaffected first-degree relatives (7,11,25 and C.D., unpublished data), which strongly suggests that the presence of monoallelic *PROKR2* mutations is not sufficient to produce the disease phenotype.

MATERIALS AND METHODS

Materials

Purified human recombinant PROK2 and the [¹²⁵I]-MIT-1 were obtained from Fitzgerald Industries International, Inc. (Concord, MA, USA) and Perkin-Elmer (Courtaboeuf, France), respectively.

Plasmids

A cDNA containing the entire coding region of the murine *Prokr2* (GenBank NM_144944) was obtained from embryonic day 10 brain RNAs, by RT-PCR using the following set of primers: *mProkr2F* 5'-CGACGCGTGGACCCAGAACAGAAACAC-3' and *mProkr2R* 5'-CTAGTCTAGACTATTTA GTCTGATACAATCC-3' (underlined sequences denote *MluI* and *XbaI* restriction sites for subsequent cloning of the PCR fragment). This PCR fragment was inserted, in place of the mGlu5-encoding *MluI-XbaI* fragment, into recombinant pRK5 plasmid vectors coding for the HA-tagged or Flag-tagged metabotropic glutamate receptor mGlu5. The final recombinant vectors code for a protein possessing the mGlu5 signal peptide followed by an N-terminal HA-tag or Flag-tag and the Prokr2 entire coding sequence. Plasmids encoding the various mutant Prokr2 harbouring each of the ten *PROKR2* missense mutations identified in KS patients were then engineered by using the QuikChange mutagenesis protocol (Stratagene, La Jolla, CA, USA).

Transfection experiments

HEK-293 cells were cultivated in Dulbecco's modified Eagle's medium supplemented with 10% fetal calf serum, and transfected by electroporation as described previously (26). In simple transfection experiments, 10⁷ cells were transfected with 2 μ g of recombinant plasmid DNA encoding either wild-type or mutant Prokr2, and completed to a total amount of 10 μ g plasmid DNA with empty pRK5 vector. In co-transfection experiments, 10⁷ cells were transfected with 0.5 and 2 μ g of the plasmids encoding the Flag-tagged wild-type Prokr2 and HA-tagged wild-type or mutant Prokr2, respectively, completed to a total amount of 10 μ g plasmid DNA with empty pRK5 vector.

Western blot analysis

Twenty hours after transfection, HEK-293 cells were washed with PBS (Ca^{2+} - and Mg^{2+} -free) and harvested. The membranes were prepared as described (26). For each sample,

30 µg of total proteins were subjected to SDS–PAGE in a 10% polyacrylamide gel. Proteins were transferred to a nitrocellulose membrane (Hybond-C; Amersham Biosciences). HA-tagged proteins were probed with a rabbit anti-HA polyclonal antibody (dilution 1/400; Zymed, San Francisco, CA, USA), and then with an Alexa-Fluor® 700 goat anti-rabbit IgG antibody (dilution 1/3000; Molecular Probes Invitrogen Corporation, Carlsbad, CA, USA). Proteins were visualized by the Odyssey® Infrared Imaging System (Li-Cor Biosciences, Lincoln, NE, USA).

Intracellular calcium measurements

After transfection, cells were seeded in polyornithine-coated, black-walled clear bottom 96-well plates, and cultivated for 20 h, as described (27). Cells were washed with freshly prepared buffer (20 mM Hepes, 1 mM MgSO₄, 3.3 mM Na₂CO₃, 1.3 mM CaCl₂, 2.5 mM probenecid, in 1 × Hank's balanced salt solution, pH 7.4) supplemented with 0.1 % bovine serum albumin, and loaded with 1 µM Ca²⁺-sensitive fluorescent dye Fluo-4 AM (Molecular Probes) for 1 h at 37°C. Cells were washed again and incubated with 50 µl of the buffer. Different concentrations of purified human PROK2 were added in the wells to reach a final volume of 100 µl, and fluorescence signals (excitation 485 nm, emission 525 nm) were measured by using the fluorescence microplate reader Flexstation (Molecular Devices) at sampling intervals of 1.5 s for 60 s. In co-transfection experiments, the calculated signalling contribution of each coexpressed receptor is the Ca²⁺ response measured when this receptor was expressed alone, divided by its cell surface amount in this condition (determined by ELISA, in arbitrary units), times its cell surface amount when it was coexpressed (ELISA, arbitrary units).

Quantification of Prokr2 at the plasma membrane by ELISA

Twenty hours after transfection, HEK-293 cells were washed with PBS and fixed with 4% paraformaldehyde in PBS for 5 min, as described (26). The cells were then either permeabilized, using 0.05% Triton X-100 for 5 min, or not permeabilized. Cells were incubated in PBS, 1% foetal calf serum (blocking solution) for 30 min. HA-tagged proteins were detected by using rat anti-HA monoclonal antibody 3F10 (Roche) at 0.5 µg/ml, and goat anti-rat IgG antibody coupled to horseradish peroxidase (Jackson Immunoresearch, West Grove, PA, USA) at 1.0 µg/ml. Flag-tagged proteins were detected with the mouse anti-Flag monoclonal antibody M2 (Sigma, St Louis, MO, USA) at 0.8 µg/ml and goat anti-mouse IgG antibody coupled to horseradish peroxidase (Amersham Biosciences, Uppsala, Sweden) at 0.25 µg/ml.

Ligand-binding assay

The ligand-binding assay was performed on intact HEK-293 cells as described (26) using 0.06 nM [¹²⁵I]-MIT-1. The radioligand was displaced by increasing concentrations of PROK2. The curves were fitted according to the equation $y = (y_{\max} - y_{\min}) / (1 + (x/IC_{50})^{nH}) + y_{\min}$ using GraphPad Prism software (San Diego), where IC₅₀ is the concentration

of the compound that inhibits 50% of bound radioligand and nH is the Hill coefficient.

Molecular modelling

Sequences of prokineticin receptors, β2 adrenergic receptor and rhodopsin, were aligned with the help of the available crystal structures (Protein Data Bank accession numbers 1gzm and 2hr1) using the program ViTO (<http://bioserv.cbs.cnrs.fr/>) (28). Molecular models of the murine Prokr2 were built using the program MODELLER 7.7 (<http://salilab.org/>) (29) with two combined templates (PDB 1gzm and PDB 2hr1) and a small set of restraints (for transmembrane helix extensions or conservation of several hydrogen bonds). Models were evaluated using ViTO and ERRAT (30).

SUPPLEMENTARY MATERIAL

Supplementary Material is available at HMG Online.

FUNDING

The work was supported by the Centre National de la Recherche Scientifique (CNRS), the Institut National de la Santé et de la Recherche Médicale (INSERM), and by grants from the French Ministry of Research, the Agence Nationale de la Recherche (ANR-BLAN06-3_135092 and ANR-05-MRAR-027-01). L.T. was supported by a fellowship from the Fondation pour la Recherche Médicale.

ACKNOWLEDGEMENTS

We thank Siluo Huang for preliminary work. This study was made possible thanks to the MTS screening facilities of the Institut Fédératif de Recherche (IFR) 3.

Conflict of Interest statement. None declared.

REFERENCES

1. Foord, S.M., Bonner, T.I., Neubig, R.R., Rosser, E.M., Pin, J.-P., Davenport, A.P., Spedding, M. and Harmar, A.J. (2005) International Union of Pharmacology. XLVI. G protein-coupled receptor list. *Pharmacol. Rev.*, **57**, 279–288.
2. Hardelin, J.-P. and Dodé, C. (2008) The complex genetics of Kallmann syndrome: *KAL1*, *FGFR1*, *FGF8*, *PROKR2*, *PROK2* et al. *Sex. Dev.*, **2**, 181–193.
3. Franco, B., Guioli, S., Pragliola, A., Incerti, B., Bardoni, B., Tonlorenzi, R., Carrozzo, R., Maestrini, E., Pieretti, M., Taillon-Miller, P. et al. (1991) A gene deleted in Kallmann's syndrome shares homology with neural cell adhesion and axonal path-finding molecules. *Nature*, **353**, 529–536.
4. Legouis, R., Hardelin, J.-P., Levilliers, J., Claverie, J.-M., Compain, S., Wunderle, V., Millasseau, P., Le Paslier, D., Cohen, D., Caterina, D. et al. (1991) The candidate gene for the X-linked Kallmann syndrome encodes a protein related to adhesion molecules. *Cell*, **67**, 423–435.
5. Dodé, C., Levilliers, J., Dupont, J.-M., De Paepe, A., Le Du, N., Soussi-Yanicostas, N., Coimbra, R.S., Delmaghani, S., Compain-Nouaille, S., Baverel, F. et al. (2003) Loss-of-function mutations in *FGFR1* cause autosomal dominant Kallmann syndrome. *Nat. Genet.*, **33**, 463–465.
6. Falardeau, J., Chung, W.C., Beenken, A., Raivio, T., Plummer, L., Sidis, Y., Jacobson-Dickman, E.E., Eliseenkova, A.V., Ma, J., Dwyer, A. et al. (2008) Decreased FGF8 signaling causes deficiency of

- gonadotropin-releasing hormone in humans and mice. *J. Clin. Invest.*, **118**, 2822–2831.
7. Dodé, C., Teixeira, L., Levilliers, J., Fouveaut, C., Bouchard, P., Kottler, M.-L., Lespinasse, J., Lienhardt-Roussie, A., Mathieu, M., Moerman, M. *et al.* (2006) Kallmann syndrome: mutations in the genes encoding prokineticin-2 and prokineticin receptor-2. *PLoS Genet.*, **2**, 1648–1652.
 8. Ng, K.L., Li, J.D., Cheng, M.Y., Leslie, F.M., Lee, A.G. and Zhou, Q.Y. (2005) Dependence of olfactory bulb neurogenesis on prokineticin 2 signaling. *Science*, **308**, 1923–1927.
 9. Matsumoto, S., Yamazaki, C., Masumoto, K.H., Nagano, M., Naito, M., Soga, T., Hiyama, H., Matsumoto, M., Takasaki, J., Kamohara, M. *et al.* (2006) Abnormal development of the olfactory bulb and reproductive system in mice lacking prokineticin receptor PKR2. *Proc. Natl Acad. Sci. USA*, **103**, 4140–4145.
 10. Pitteloud, N., Zhang, C., Pignatelli, D., Li, J.D., Raivio, T., Cole, L.W., Plummer, L., Jacobson-Dickman, E.E., Mellon, P.L., Zhou, Q.Y. *et al.* (2007) Loss-of-function mutation in the prokineticin 2 gene causes Kallmann syndrome and normosmic idiopathic hypogonadotropic hypogonadism. *Proc. Natl Acad. Sci. USA*, **104**, 17447–17452.
 11. Cole, L.W., Sidis, Y., Zhang, C., Quinton, R., Plummer, L., Pignatelli, D., Hughes, V.A., Dwyer, A.A., Raivio, T., Hayes, F.J. *et al.* (2008) Mutations in prokineticin-2 (PROK2) and PROK2 receptor-2 (PROKR2) in human gonadotrophin-releasing hormone deficiency: molecular genetics and clinical spectrum. *J. Clin. Endocrinol. Metab.*, **93**, 3551–3559.
 12. Palczewski, K., Kumasaka, T., Hori, T., Behnke, C.A., Motoshima, H., Fox, B.A., Le Trong, I., Teller, D.C., Okada, T., Stenkamp, R.E. *et al.* (2000) Crystal structure of rhodopsin: a G protein-coupled receptor. *Science*, **289**, 739–745.
 13. Li, J., Edwards, P.C., Burghammer, M., Villa, C. and Schertler, G.F. (2004) Structure of bovine rhodopsin in a trigonal crystal form. *J. Mol. Biol.*, **343**, 1409–1438.
 14. Rosenbaum, D.M., Cherezov, V., Hanson, M.A., Rasmussen, S.G., Thian, F.S., Kobilka, T.S., Choi, H.J., Yao, X.J., Weis, W.I., Stevens, R.C. *et al.* (2007) GPCR engineering yields high-resolution structural insights into beta2-adrenergic receptor function. *Science*, **318**, 1266–1273.
 15. Cherezov, V., Rosenbaum, D.M., Hanson, M.A., Rasmussen, S.G., Thian, F.S., Kobilka, T.S., Choi, H.J., Kuhn, P., Weis, W.I., Kobilka, B.K. *et al.* (2007) High-resolution crystal structure of an engineered human beta2-adrenergic G protein-coupled receptor. *Science*, **318**, 1258–1265.
 16. Ballesteros, J.A. and Weinstein, H. (1995) Integrated methods for the construction of three-dimensional models and computational probing of structure-function relations in G-protein coupled receptors. *Methods Neurosci.*, **25**, 366–428.
 17. Lin, D.C., Bullock, C.M., Ehler, F.J., Chen, J.L., Tian, H. and Zhou, Q.Y. (2002) Identification and molecular characterization of two closely related G protein-coupled receptors activated by prokineticins/endocrine gland vascular endothelial growth factor. *J. Biol. Chem.*, **277**, 19276–19280.
 18. Masuda, Y., Takatsu, Y., Terao, Y., Kumano, S., Ishibashi, Y., Suenaga, M., Abe, M., Fukusumi, S., Watanabe, T., Shintani, Y. *et al.* (2002) Isolation and identification of EG-VEGF/prokineticins as cognate ligands for two orphan G-protein-coupled receptors. *Biochem. Biophys. Res. Commun.*, **293**, 396–402.
 19. Soga, T., Matsumoto, S., Oda, T., Saito, T., Hiyama, H., Takasaki, J., Kamohara, M., Ohishi, T., Matsushime, H. and Furuichi, K. (2002) Molecular cloning and characterization of prokineticin receptors. *Biochim. Biophys. Acta*, **1579**, 173–179.
 20. Bullock, C.M., Li, J.D. and Zhou, Q.Y. (2004) Structural determinants required for the bioactivities of prokineticins and identification of prokineticin receptor antagonists. *Mol. Pharmacol.*, **65**, 582–588.
 21. Samson, M., Libert, F., Doranz, B.J., Rucker, J., Liesnard, C., Farber, C.M., Saragosti, S., Lapoumeroulie, C., Cognaux, J., Forceille, C. *et al.* (1996) Resistance to HIV-1 infection in caucasian individuals bearing mutant alleles of the CCR-5 chemokine receptor gene. *Nature*, **382**, 722–725.
 22. Benkirane, M., Jin, D.Y., Chun, R.F., Koup, R.A. and Jeang, K.T. (1997) Mechanism of transdominant inhibition of CCR5-mediated HIV-1 infection by ccr5delta32. *J. Biol. Chem.*, **272**, 30603–30606.
 23. Kaykas, A., Yang-Snyder, J., Heroux, M., Shah, K.V., Bouvier, M. and Moon, R.T. (2004) Mutant Frizzled 4 associated with vitreoretinopathy traps wild-type Frizzled in the endoplasmic reticulum by oligomerization. *Nat. Cell Biol.*, **6**, 52–58.
 24. Dodé, C. and Hardelin, J.-P. (2008) Kallmann syndrome. *Eur. J. Hum. Genet.* (in press).
 25. Abreu, A., Trarbach, E., de Castro, M., Frade Costa, E., Versiani, B., Matias Baptista, M., Mendes Garmes, H., Bilharinho Mendonca, B. and Latronico, A. (2008) Loss-of-function mutations in the genes encoding prokineticin-2 or prokineticin receptor-2 cause autosomal recessive Kallmann syndrome. *J. Clin. Endocrinol. Metab.* (in press).
 26. Liu, J., Maurel, D., Etzol, S., Brabet, I., Ansanay, H., Pin, J.-P. and Rondard, P. (2004) Molecular determinants involved in the allosteric control of agonist affinity in the GABA-B receptor by the GABA-B2 subunit. *J. Biol. Chem.*, **279**, 15824–15830.
 27. Goudet, C., Gaven, F., Kniazeff, J., Vol, C., Liu, J., Cohen-Gonsaud, M., Acher, F., Prézeau, L. and Pin, J.-P. (2004) Heptahelical domain of metabotropic glutamate receptor 5 behaves like rhodopsin-like receptors. *Proc. Natl Acad. Sci. USA*, **101**, 378–383.
 28. Catherinot, V. and Labesse, G. (2004) ViTO: tool for refinement of protein sequence-structure alignments. *Bioinformatics*, **20**, 3694–3696.
 29. Sali, A. and Blundell, T.L. (1993) Comparative protein modelling by satisfaction of spatial restraints. *J. Mol. Biol.*, **234**, 779–815.
 30. Colovos, C. and Yeates, T.O. (1993) Verification of protein structures: patterns of nonbonded atomic interactions. *Protein Sci.*, **2**, 1511–1519.